Integrated Ferroelectrics, 123:10–17, 2011

ISSN: 1058-4587 print / 1607-8489 online
DOI: 10.1080/10584587.2011.570586

Taylor & Francis
Taylor & Francis Group

First-Principles Modeling of Oxygen Interaction with $SrTiO_3$(001) Surface: Comparative Density-Functional LCAO and Plane-Wave Study

VITALY ALEXANDROV,[1] SERGEI PISKUNOV,[2,3,4,*]
YURI F. ZHUKOVSKII,[4] EUGENE A. KOTOMIN,[4,5]
AND JOACHIM MAIER[5]

[1]Department of Chemical Engineering and Materials Science and NEAT ORU, University of California, 1 Shields Avenue, Davis, California 95616-5294, USA
[2]Faculty of Computing, University of Latvia, 19 Raina blvd., Riga, LV-1586, LATVIA
[3]Faculty of Physics and Mathematics, University of Latvia, 8 Zellu Str., Riga, LV -1002, LATVIA
[4]Institute for Solid State Physics, University of Latvia, 8 Kengaraga Str., Riga, LV -1063, LATVIA
[5]Max-Planck-Institute for Solid State Research, Heisenbergsrtr. 1, Stuttgart 70569, GERMANY

Large scale first-principles calculations based on density functional theory (DFT) employing two different methods (atomic orbitals and plane wave basis sets) were used to study the energetics, geometry, the electronic charge redistribution and migration for adsorbed atomic and molecular oxygen on defect-free $SrTiO_3$(001) surfaces (both SrO- and TiO_2-terminated), which serves as a prototype for many ABO_3-type perovskites. Both methods predict substantial binding energies for atomic O adsorption at the bridge position between the oxygen surface ions and an adjacent metal ion. A strong chemisorption is caused by formation of a surface molecular peroxide ion. In contrast, the neutral molecular adsorption energy is much smaller, ∼0.25 eV. Dissociative molecular adsorption is energetically unfavorable, even at 0 K. Adsorbed O atoms migrate along the (001) direction with an activation energy of ∼1 eV which is much larger than that for surface oxygen vacancies (0.14 eV). Therefore, the surface O vacancies control encounter with the adsorbed O atoms and oxygen penetration to the surface which is the limiting step for many applications of ABO_3-type perovskites, including resistive oxygen sensors, permeation ceramic membranes and fuel cell technology.

Introduction

The interaction of gas-phase oxygen with the perovskite surfaces is important for the fundamental understanding of oxide reactivity and for many applications involving permeation membrane technology, sensors, capacitors, photocatalysts, as well as fuel cell electrodes [1, 2]. The difficulties of distinguishing between adsorbed and lattice oxygen (unless the adsorbed species carry a net spin) result in a significant lack of experimental information

Received May 19, 2010; in final form June 25, 2010.
*Corresponding author. E-mail: piskunov@lu.lv

about the oxygen adsorption processes occurring on perovskite surfaces. Also, the *ab initio* simulations of oxygen adsorption on ABO_3 perovskites are very scarce in the literature. Recently, we reported first principles calculations for surfaces of Sr-doped $LaMnO_3$ [3] used as fuel cell cathodes.

In this paper, we present results of large-scale calculations of adsorption and diffusion of atomic and molecular oxygen on the (001) surface of a cubic $SrTiO_3$ which serves as a prototype for a wide class of ABO_3 perovskites. We use two different versions of the first principles DFT approaches which are discussed below. The main questions that we want to answer in our comparative study were the following: (*i*) which adsorption sites are most energetically favorable, (*ii*) what is the nature of bonding of adsorbed oxygen atoms and molecules to the $SrTiO_3$ surfaces, (*iii*) what is the diffusion mechanism of the adsorbed species, (iv) what is the difference in mobilities of adsorbed oxygens and surface vacancies, (v) how a choice of the two different calculation methods affects the results.

Computational Details

In our comparative study we have used two quite different DFT approaches: the *hybrid* exchange-correlation functional with optimized LCAO (linear combination of atomic orbitals) basis set (BS) and the generalized gradient approximation (GGA) with plane-wave (PW) BS. To perform hybrid calculations, we have used the *CRYSTAL* computer code (see [4] and references therein). This code employs the Gaussian-type functions for an expansion of the crystalline orbitals. The BSs used in this study were carefully optimized by us elsewhere [5]: O 8–411(1d)G, Ti 411(311d)G, and Sr 311(1d)G, whereby inner core electrons of Sr and Ti atoms are described by Hay-Wadt effective core potentials [6]. The exchange-correlation B3PW functional [7] involves a hybrid of non-local HF exact exchange and exchange potentials constructed using both Local Density Approximation (LDA) and non-local GGA, combined with the GGA correlation potential of Perdew and Wang. Our previous studies show that the B3PW exchange-correlation technique is a reliable tool to calculate both surface properties and electronic structure of defective ABO_3 perovskites [8]. This gives us a firm ground to adopt the B3PW hybrid functional in the present study of oxygen adsorption on the $SrTiO_3$ (001) surfaces. Preliminary *CRYSTAL* calculations were discussed in Ref. [9].

In our PW simulations on $SrTiO_3$(001) surfaces, we have used the *VASP 4.6* code [10], with the PBE-GGA nonlocal functional [11] employed for both exchange and correlation. The cut-off energy was chosen to be 400 eV. The vacuum gap along the z axis was chosen 19.5 Å.

We considered both SrO- and TiO_2-terminated $SrTiO_3$(001) surfaces. These were modeled using 7-layer symmetrically terminated slab unit cells [12]. In order to simulate the isolated adsorbed species, the aforementioned slab unit cell was extended in *CRYSTAL* calculations to a 2×2 slab surface supercell. The reciprocal space integration was performed by sampling of the Brillouin zone (BZ) of the supercell with the $6 \times 6 \times 1$ Pack-Monkhorst net [13] which provides a balanced summation over the direct and reciprocal lattices. In the VASP calculations $2\sqrt{2} \times 2\sqrt{2}$ primitive unit cells corresponding to 12.5% surface defect coverage and a $2 \times 2 \times 1$ Monkhorst-Pack mesh of k points [13] was used. The initial guess for relaxation of bare $SrTiO_3$(001) surfaces was taken from [12], further optimization was performed using analytical methods as implemented in both *VASP* and *CRYSTAL* codes (including nudged elastic band method (NEB) in the VASP [14, 15]). To save the computational time and due to problems with convergence for fully relaxed structures, in the LCAO calculations of O adsorbed atop surface Ti and Sr ions, the O-Me atoms were

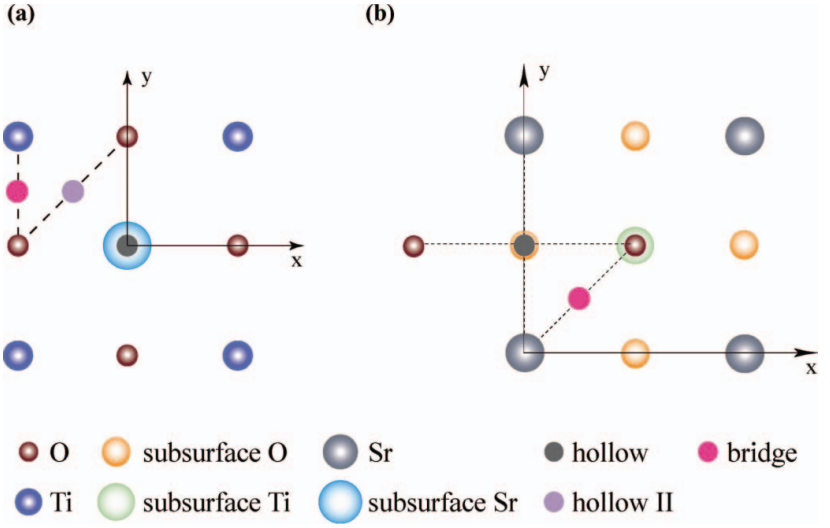

Figure 1. Top views of the possible positions for oxygen adsorption on (a) TiO_2- and (b) SrO-terminated (001) substrate (see labels).

fixed at positions obtained in the PW calculations to preserve their interatomic distance, while all other ions were allowed to relax.

In order to obtain an overall picture of the equilibrium geometry, energetics, and the electronic structure, we have studied the adsorption of atomic oxygen at a variety of sites on the relaxed but unreconstructed cubic SrO- and TiO_2-terminated $SrTiO_3(001)$ surfaces as shown at Figure 1. Oxygen atom adsorption energies were calculated with respect to the energy of an oxygen free atom in the triplet ground state:

$$E_{ads}^{(at)} = -\frac{1}{2}\left(E_{tot}^{system} - E_{tot}^{slab} - 2E_{tot}^{O_{triplet}}\right). \quad (1)$$

where E_{tot}^{slab} is the total energy of fully relaxed substrate slab, $E_{tot}^{O_{triplet}}$ is the energy of an isolated oxygen atom in the ground triplet state, and E_{tot}^{system} is the energy of a slab containing an adsorbate. The prefactors 1/2 and co-factor of 2 before $E_{tot}^{O_{triplet}}$ appear since the interface is modeled by a substrate slab with two equivalent surfaces and two O_{ads} atoms symmetrically positioned on both sides of slab. If E_{ads} is positive, the adsorption is energetically favorable.

Results and Discussion

Adsorption of Atomic Oxygen

Table I comprises the calculated O atom adsorption energies (with respect to a free O atom in the triplet state) for all five surface sites under consideration (Fig. 1). Both methods predict the most favorable configurations of oxygen adsorption on both surface terminations to be the *bridge position*. The calculated binding energies are typically larger in the PW method.

Table 1
The oxygen adsorption energies (in eV) from eq. (1) calculated using the PW-PBE method (VASP code) and the LCAO-B3PW (CRYSTAL code). The adsorbed oxygen atom at the hollow sites was considered in the ground (triplet) state. The energetically most favorable positions are given in bold.

Site	PW-PBE	LCAO-B3PW	Site	PW-PBE	LCAO-B3PW
TiO_2-termination			SrO-termination		
Ti	2.13	0.70	Sr	0.57	0.37
O	2.51	1.76	O	2.44	1.54
Bridge	**2.96**	**2.03**	Bridge	**3.06**	**2.43**
Hollow	1.12	0.93	Hollow	1.73	1.08

The analysis of the interatomic distances (Table II) indicates that at the bridge position the adatom is substantially shifted towards the nearest surface metal atom. A further analysis by means of the effective atomic charges (Bader and Mulliken approaches, Table III) along with the electron density maps (Fig. 2) points at the formation of pseudo-molecular tilted species O_{ads}-O_{surf} (peroxide O_2^{2-} ion).

The redistribution of the electron density in the vicinity of the adsorbed oxygen atom (Fig. 2) was obtained within the hybrid HF-DFT method, while it is known that the pure DFT approach commonly overestimates the covalent contribution in the chemical bonding. This also explains the generally larger adsorption energies obtained within the pure DFT method (PW-PBE) (Table I).

Nevertheless, both methods draw the same conclusions about the atomic oxygen adsorption on the surfaces of $SrTiO_3$ crystal. Specifically, (*i*) there is a strong chemisorption with the highest adsorption energy for the bridge position; (*ii*) O_{ads} is bound stronger on the more ionic SrO surface than on the TiO_2 termination.

Table 2
Distances (in Å) between the adsorbed oxygen atom and the nearest O_s and Ti_s (or Sr_s) atoms for optimized adsorption structures of $SrTiO_3$ (001) substrates.

	PW-PBE		LCAO-B3PW	
Site	O_{surf}	$Ti(Sr)_{surf}$	O_{surf}	$Ti(Sr)_{surf}$
TiO_2-termination				
Ti	2.45	1.65	2.45	1.65
O	1.45	2.31	1.46	2.76
Bridge	1.46	1.56	1.47	1.91
Hollow	2.43	3.18	2.24	2.00
SrO-termination				
Sr	3.32	2.33	3.32	2.33
O	1.47	2.85	1.47	3.24
Bridge	1.49	2.09	1.50	2.45
Hollow	2.62	2.47	2.48	2.53

Table 3

The effective atomic charges, in *e* (Bader analysis in PW-PBE and Mulliken analysis in LCAO-B3PW), for the adsorbed oxygen atom and the nearest surface O and Ti (or Sr) atoms for optimized adsorption structures of $SrTiO_3$ (001) substrates. Atomic charges at the defect-free surface layer are: PW-PBE: Ti 2.03, O −1.16e (TiO_2 termination); Sr 1.56, O −1.28e (SrO termination); LCAO-B3PW: Ti 2.31, O −1.32e; Sr 1.84, O −1.52e.

	PW-PBE			LCAO-B3PW		
Site	O_{ads}	O_{surf}	$Ti(Sr)_{surf}$	O_{ads}	O_{surf}	$Ti(Sr)_{surf}$
TiO_2-termination						
Ti	−0.76	−1.12	2.03	−0.60	−1.10	2.39
O	−0.61	−0.69	2.05	−0.62	−0.77	2.29
Bridge	−0.49	−0.71	2.13	−0.52	−0.79	2.28
Hollow	−0.23	−1.13	2.02	−0.29	−1.16	2.29
SrO-termination						
Sr	−0.71	−1.22	1.54	−0.65	−1.32	1.87
O	−0.73	−0.80	1.58	−0.71	−0.90	1.86
Bridge	−0.79	−1.07	1.56	−0.84	−0.88	1.85
Hollow	−0.72	−1.12	1.59	−0.52	−1.32	1.86

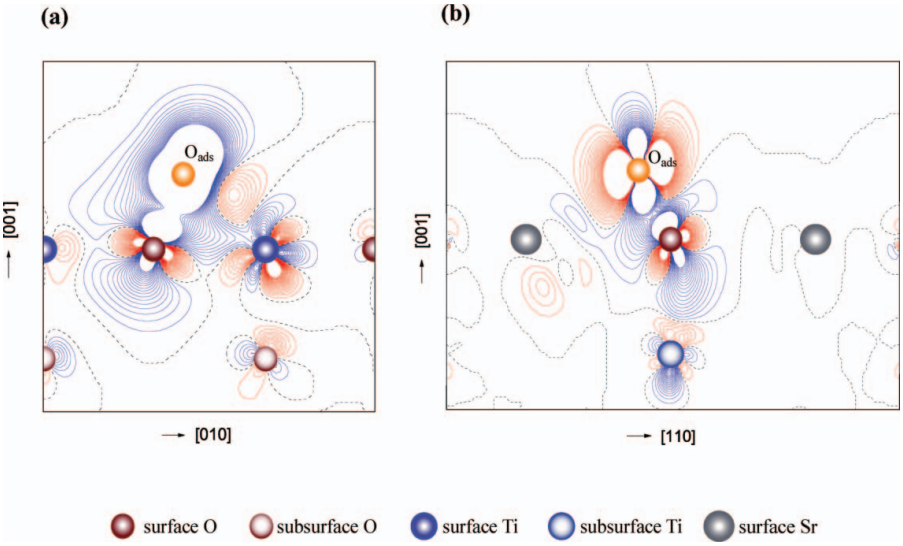

Figure 2. The differential electron density maps (the total density of the surface containing an adsorbate minus the sum of the electron densities of both isolated oxygen atom and bare slab) for O_{ads} over the bridge position on (a) TiO_2-terminated and (b) SrO-terminated surfaces. On the electron density map, solid (red), dash (blue) and dash-dot (black) lines describe positive, negative and zero values of the induced electron density, respectively.

In both methods the energy gain due to adsorption of two oxygen atoms is smaller than the free molecule dissociation energy (experimental value 5.12 eV [16], cf. with calculated values of 5.30 eV LCAO and 6.05 eV PW-PBE). Therefore, dissociation of oxygen molecule due to adsorption on a defect-free surface is energetically unfavorable.

Adsorption of Molecular Oxygen

We explored a number of possible sites and orientations for the adsorption of an O_2 molecule on both terminations of $SrTiO_3(001)$. (Note that the LCAO-calculated bond lengths of a free O_2 molecule are 1.20 Å and 1.23 Å for LCAO and PW methods, in good agreement with experiment, 1.21 Å [16]). The LCAO calculations show that molecular adsorption occurs at hollow sites (hollow II for TiO_2 termination as shown in Fig. 1) with the molecular axis oriented perpendicular to the surface. The relevant adsorption energies E_{ads} are 0.02 and 0.09 eV for SrO- and TiO_2- terminated $SrTiO_3(001)$ surfaces, respectively.

In turn, the PW-PBE method yields the largest $E_{ads} = 0.25$ eV for the bridge position between Ti and O surface atoms at the TiO_2-terminated surface (the molecular axis is just slightly tilted from normal vector toward surface O atom). In both the LCAO and the PW-PBE methods the equilibrium distance between surface and molecular adsorbate is found to be as large as $\sim$3 Å. The Mulliken population analysis shows practically no charge transfer between the surface atoms and adsorbate. This fact and invariance of the O_2 bond length, demonstrate that we are dealing with quite weak physisorption.

Diffusion of Oxygen Species

The limiting step for many perovskite applications (e.g. fuel cells and permeation membranes) is the penetration of the adsorbed oxygen atom into the nearby surface oxygen vacancy. The kinetics of this process is controlled by mutual encounter of the two species and thus needs calculation of the migration energies of both adsorbed O atoms and oxygen vacancies. First of all, it follows from the Table 1 that the migration energy of the adsorbed oxygen between the most energetically favorable bridge positions along the (100) direction via the position above Ti ions on the TiO_2-terminated surface requires 0.83 eV according to the *VASP* and 1.33 eV in the *CRYSTAL* calculations. (The main discrepancy stems from the low binding energy predicted for O atop Ti in the latter calculations, one of reasons could be non-optimized Ti-O distance).

On the SrO terminated surface, the migration occurs along the (110) directions with the hollow position as the saddle point. The relevant energies are very close, 1.33 eV and 1.35 eV for *VASP* and *CRYSTAL*, respectively. These energies are larger than those for TiO_2 termination due to a larger O binding energy resulting from more negative O ions on the SrO surface (Table 3). Recent VASP calculations [17] show the same trend, 0.81 eV and 0.68 eV for SrO and TiO_2 terminations, though the absolute values which differ from our study, probably due to larger supercells used there.

Another step was the calculation of the O *vacancy* migration energy along the TiO_2 (001) surface using the VASP code. The value of the barrier is expected to be lower than that for the bulk because of the reduced coordination number for surface atoms. Our calculations show that the barrier is indeed 0.14 eV, being almost by a factor three lower than that calculated for the bulk (0.38 eV). Note that the bulk value is too low as compared to the experimental data (0.86 eV [18]). The reason could be that we treated a neutral vacancy (electron density from missing O *atom* is trapped by two nearest Ti ions) whereas experiments refer to the charged vacancies at high temperatures (electrons trapped

somewhere in crystal far from a vacancy). Our energies are similar to another VASP study [19] (see also review article [8]). Thus, we predict highly mobile surface oxygen vacancies as compared to the vacancies in the bulk as well as adsorbed O atoms.

Lastly, computer simulations of the adsorbed oxygen atom dropping into the closest oxygen vacancy reveal a distinguishable but extremely small activation barrier, just 0.01 eV. Hence, we predict an almost no-barrier penetration of the adsorbed O atom into the nearby vacancy that occurs when the strongly-bound adatom meets the very mobile surface oxygen vacancy.

Conclusions

We have performed a number of first-principles calculations on a cubic $SrTiO_3(001)$ substrate containing oxygen adsorbates. In our modeling we have applied two different approaches, LCAO-B3PW and PW-PBE within density functional theory. Both approaches predict that the most favorable adsorption sites for oxygen atoms are bridge positions on both terminations. On the SrO-terminated substrates, the oxygen adatom is bound more strongly than on TiO_2-terminated one. Our calculations show that the O_{ads} atoms tend to form the molecular peroxide ions with surface oxygens which is consistent with a recent VASP study [17]. In contrast, on a clean defect-free $SrTiO_3(001)$ substrate, molecular adsorption is very weak.

The diffusion of atomic oxygen along the surfaces is expected to have relatively high activation energies and to be quite anisotropic. We predict almost barrier-free penetration of the adsorbed O ions into the much more mobile surface vacancies, similarly to what we found recently for $LaMnO_3$ [3,15]. This demonstrates that a high concentration of mobile vacancies is important for high performance of ceramic membranes for gas separation or for fuel cell electrodes. A DFT study of more complex perovskite materials such as $(Ba,Sr)(Co,Fe)O_3$ (BSCF) is in progress.

Acknowledgments

Many thanks to R. Merkle, E. Heifets and Yu. Mastrikov for numerous stimulating discussions. This study has been partly supported through the European Social Fund (ESF) project Nr. 2009/0216/1DP/1.1.1.2.0/09/APIA/VIAA/044 and EC FP7 NASA-OTM project under grand agreement No. 228701. VA thanks the Max Planck Institute for Solid State Research and its International School for Advanced Materials for financial support and hospitality during his PhD study.

References

1. C. Noguera, Physics and Chemistry of Oxide Surfaces, New York: Cambridge Univ. Press; 1996.
2. R. Merkle and J. Maier, How is Oxygen Incorporated into Oxides? *Angew. Chem. Int. Ed.* **47**, 2–23 (2008).
3. Yu. Mastrikov, R. Merkle, E. Heifets, E. A. Kotomin, and J. Maier, Pathways for oxygen incorporation in mixed conducting pervoskites. *J. Phys. Chem. C* **114**, 3017–3027 (2010).
4. R. Dovesi, V. R. Saunders, C. Roetti, R. Orlando, C. M. Zicovich-Wilson, F. Pascale, B. Civalleri, K. Doll, N. M. Harrison, I. J. Bush, Ph. D'Arco, and M. Llunell, *CRYSTAL-2006 User's Manual*, University of Torino, Torino; 2006. http://www.crystal.unito.it/
5. S. Piskunov, E. Heifets, R. I. Eglitis, and G. Borstel, Bulk properties and electronic structure of $SrTiO_3$, $BaTiO_3$, $PbTiO_3$ perovskites: an ab initio HF/DFT study. *Comp. Mat. Sci.* **29**, 165–178 (2004).

6. P. J. Hay and W. R. Wadt, *Ab initio* effective core potentials for molecular calculations. Potentials for K to Au including the outermost core orbitals. *J. Chem. Phys.* **82**, 299–310 (1984).
7. A. D. Becke, Density-functional thermochemistry. III. The role of exact exchange. *J. Chem. Phys.* **98**, 5648–5652 (1993).
8. Yu. F. Zhukovskii, E. A. Kotomin, R. A. Evarestov, and D. E. Ellis, Periodic models in quantum chemical simulations of F centers in crystalline metal oxides. *Int. J. Quant. Chem.* **107**, 2956–2985 (2007).
9. S. Piskunov, Yu. F. Zhukovskii, E. A. Kotomin, E. Heifets, and D. E. Ellis, *MRS Proc.* **894**, LL08-05-1-6 (2006).
10. G. Kresse, M. Marsman, and J. Furthmüller, *VASP* the Guide. University of Vienna, Austria; 2009.
11. J. P. Perdew, K. Burke, and M. Ernzerhof, Generalized gradient approximation made simple. *Phys. Rev. Lett.* **77**, 3865–3868 (1996).
12. S. Piskunov, E. A. Kotomin, E. Heifets, J. Maier, R. I. Eglitis, and G. Borstel, Hybrid DFT calculations of the atomic and electronic structure for ABO_3 perovskite (001) surfaces. *Surf. Sci.* **575**, 75–88 (2005).
13. H. J. Monkhorst and J. D. Pack, Special points for Brillouin-zone integrations. *Phys. Rev. B* **13**, 5188–5192 (1976).
14. G. Henkelman, B. Uberuaga, and H. Jonsson, A climbing image nudged elastic band method for finding saddle points and minimum energy paths. *J Chem. Phys.* **113**, 9901–9904 (2000).
15. E. A. Kotomin, Y. A. Mastrikov, E. Heifets, and J. Maier, Adsorption of atomic and molecular oxygen on the $LaMnO_3(001)$ surface: *Ab initio* supercell calculations and thermodynamics. *Phys. Chem. Chem. Phys.* **10**, 4644–4649 (2008).
16. D. R. Lide, CRC Handbook of Chemistry and Physics, 74th ed.: CRC Press, Boca Raton, FL; 1993.
17. H. Guhl, W. Miller, and K. Reuter, Oxygen adatoms at $SrTiO_3(001)$: A density-functional theory study. *Surf. Sci.* **604**, 372–376 (2010).
18. I. Denk, W. Munch, and J. Maier, Partial conductivities in $SrTiO_3$: Bulk polarization experiments, oxygen concentration cell measurements and defect-chemical modeling. *J. Am. Cer. Soc.* **78**, 3265–3269 (1995).
19. J. Carrasco, F. Illas, N. Lopez, E. A. Kotomin, Yu. F. Zhukovskii, R. A. Evarestov, Yu. Mastrikov, S. Piskunov, and J. Maier, First-principles calculations of the atomic and electronic structure of *F* centers in the bulk and on the (001) surface of $SrTiO_3$. *Phys. Rev. B* **73**, 054106-1-11 (2006).